SOURCE-GENERATED NOISE IN SHALLOW SEISMIC DATA

JOHAN O.A. ROBERTSSON, KLAUS HOLLIGER and ALAN G. GREEN

Institute of Geophysics, ETH-Hönggerberg, CH-8093 Zürich, Switzerland.

(Received January 12, 1996; revised version accepted May 14, 1996)

ABSTRACT

Robertsson, J.O.A., Holliger, K. and Green, A.G., 1996. Source-generated noise in shallow seismic data. *European Journal of Environmental and Engineering Geophysics*, 1: 107-124.

To simulate seismic images of a highly heterogeneous and anelastic shallow subsurface requires full waveform techniques that properly account for scattering and attenuation. A viscoelastic finite-difference technique is employed to quantify the effects that typical near-surface features (i.e., approximately the uppermost 20 m) have on high-resolution seismic refraction and reflection data. Guided waves, ground roll and energy scattered from shallow heterogeneities and surface topography are forms of source-generated noise that may affect data quality. Dispersion of guided waves narrows the 'optimum reflection window' between the first arrivals and the ground roll, and the intrinsically shingled nature of guided waves may lead to mis-picking of first breaks for refraction analyses and difficulties in identifying and processing shallow reflections. Numerical modeling demonstrates that even minor topographic features may cause significant scattering of guided waves and ground roll from the earth's surface. The scattered energy appears as ubiquitous source-generated noise that interferes with reflections and diffractions throughout the seismic record. The amount of noise generated by this scattering mechanism, and thus its impact on the imaging of subsurface structures, depends critically on the degree of attenuation in the uppermost layers.

KEY WORDS: numerical modeling, high-resolution seismology, viscoelasticity, source-generated noise, attenuation, finite-difference method, topography, near-surface effects, guided waves.

1359-8155/96/$5.00

INTRODUCTION

Seismic and other geophysical investigations of the environmentally sensitive near-surface regions of the earth have increased enormously over the past decade in connection with groundwater monitoring, resource exploration and engineering (including waste disposal) activities (Ward, 1990). The principal goal of most shallow seismic surveys is to map the upper 50-100 m of the underground with a resolution of a few metres (Steeples et al., 1995a). In general, the resolving power of the seismic reflection technique is limited by the dominant wavelengths of the reflected signal. An additional limitation arises when there is a need to image very near-surface features (approximately within the upper 20 m). Reflections from such features are best observed in a limited offset-time window that is bounded above by the direct, refracted and guided waves and below by the shear waves, ground roll and air waves (Fig. 1; Robertsson et al., 1996). The resolving power in the upper parts of a seismic

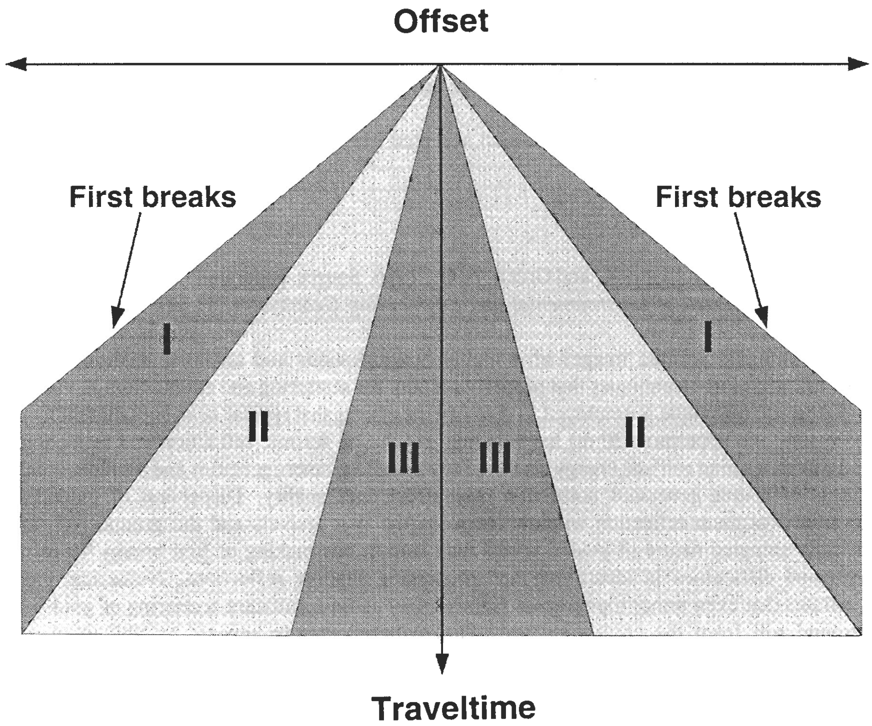

Fig. 1. Schematic illustration of a typical high-resolution seismic shot record. I is first-break zone that includes high-amplitude shingled guided waves; II is quiet zone ('optimum reflection window') in which desired reflections are mostly observed - may be contaminated with scattered energy generated by interaction of guided waves with shallow heterogeneities and minor topographic features; III is zone dominated by shear waves, dispersive and multiply scattered high-amplitude ground roll, and air waves.

reflection section is thus not only dependent on the wavelength of the signal, but also, and generally more critically, on the effects of so-called source-generated noise. Prominent forms of source-generated noise include guided waves, shear waves, ground roll, air waves and energy scattered from near-surface heterogeneities and surface relief.

Seismic impedance contrasts associated with the thin blanket of unconsolidated sediments that cover much of the earth's continents are often large, comparable in many regions to those observed at the seafloor and at the crust-mantle discontinuity. Further, the near-surface region is commonly highly heterogeneous and the scales of topographic relief are often comparable to the seismic wavelengths of interest. Whereas the effects of shear waves, ground roll and air waves are easily identified and relatively well understood, those of guided waves and scattering from surface topography and shallow heterogeneity are not (Fig. 1). Recently, Robertsson et al. (1996) have demonstrated that waveguides formed between the earth's surface and sharp P-velocity contrasts within or bounding the surficial sediments may significantly affect the quality of high-resolution seismic refraction and reflection data.

Within this paper, after reviewing the seismic properties of unconsolidated surficial sediments (approximately upper 20 m; Stümpel et al., 1984; Hübner et al., 1985), the conditions required for the formation of near-surface waveguides will be summarised (Robertsson et al., 1996). Then, a two-dimensional (2-D) viscoelastic finite-difference scheme (Robertsson et al., 1994) will be used to quantify the effects of: (i) scattering from gentle topographic variations, (ii) near-surface waveguides with and without topographic relief, and (iii) varying degrees of attenuation within the waveguide. Finally, the synthetic data will be compared to a typical high-resolution shot record.

THE NEAR-SURFACE ENVIRONMENT

Unconsolidated surficial sediments commonly include gravel, sand, silt and clay with P-velocities ranging from about 250 m/s to 3000 m/s (i.e. 2.5 - 30 m wavelengths at 100 Hz), S-velocities below 500 m/s, and poorly known, but generally high-attenuation properties (Hübner et al., 1985; Steeples et al., 1995b). Velocities in this zone are influenced by sediment lithology, porosity and water content. *In situ* borehole measurements (see Fig. 2 (Stümpel et al., 1984)) reveal the wide range of velocities (500 to 3000 m/s) that may be associated with sand and boulder clay. These data also illustrate how water saturation of sand leads to sharp increases in P-velocities without appreciably affecting S-velocities. Laboratory measurements also demonstrate that very abrupt increases in P-velocity occur as sand approaches a state of complete water saturation (e.g. Hübner et al., 1985).

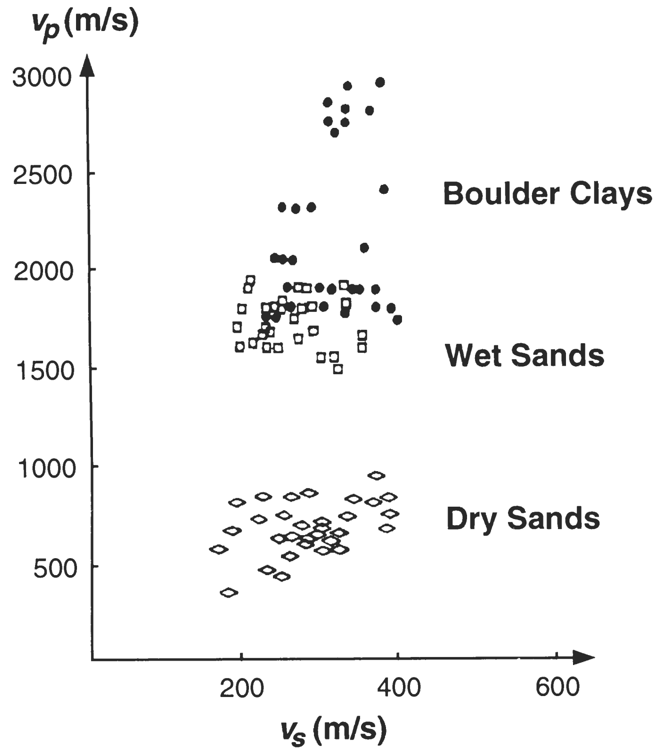

Fig. 2. *In situ* borehole measurements of P- and S-velocities for boulder clay, water-saturated sands, and dry to partially saturated sands reduced to a pressure of 0.1 MPa, which is equivalent to about 4 m depth (from Stümpel et al., 1984).

NEAR-SURFACE WAVEGUIDES: RESULTS FROM SIMPLE MODAL CALCULATIONS

On the basis of a simple modal analysis of wave propagation in layered homogeneous acoustic media, it can be shown that the cut-off frequency f_l of mode l in a near-surface waveguide is described by

$$f_l = c(l + 1/2) / 2h\sqrt{(1 - n^2)} \quad , \quad l = 0, 1, 2, \ldots, \tag{1}$$

where c and h are the P-velocity and thickness, respectively, of the waveguide, $n = c/c_1$ the refractive index at its base, and c_1 the P-velocity in the underlying medium. Strong channelling of energy will occur within the waveguide when the dominant seismic frequencies fall within the lowermost mode (i.e., between the cut-off frequencies of the 0th and 1st normal modes). The generation of guided waves results in the effective extraction of energy from the transmitted wavefield, which in turn leads to generally weaker reflections from below the waveguide (Robertsson et al., 1996). In addition, the resultant package of shingled guided waves may mask the shallow reflections.

Impedance discontinuities that may form the lower boundary of a shallow waveguide include the unconsolidated sediment-bedrock contact and the ground-water table. For example, an efficient waveguide would be expected in regions where P-velocities of unconsolidated sediments lie between 250 and 1500 m/s and where the ground-water table occurs at depths of 3-15 m (Robertsson et al., 1996). A waveguide formed under these conditions, which are common to temperate regions of the earth, would affect seismic energy in the 30 and 500 Hz band, the dominant frequency range of many high-resolution seismic sources (e.g., hammers, shotguns or mini-vibroseis; Miller et al. (1994) and references therein; Matsubara et al., 1995). Clearly, excitation of the earth under a broad range of near-surface conditions will result in significant source-generated noise in the form of shingled guided waves. Although the following analysis will be concerned with waveguides formed between the earth's surface and the ground-water table, the results are applicable to any other environment with a shallow waveguide.

The phase velocity for the l-th normal mode, v_l, decreases monotonically with wavenumber, k (Robertsson et al., 1996). The group velocity, u_l, can be calculated from the relation (Brekhovskikh, 1980):

$$u_l(k) = v_l + k(\partial v_l/\partial k) \quad . \tag{2}$$

Since the derivative in equation (2) is invariably negative, the group velocity is always lower than the phase velocity and lower than c. As discussed below, this may have implications for the interpretation of high-resolution seismic data.

VISCOELASTIC FINITE-DIFFERENCE SCHEME

The finite-difference technique employed in this work is based on a staggered stress-velocity formulation of the first-order partial differential equations that describe wave propagation in 2-D viscoelastic media (Robertsson et al., 1994). It is second-order accurate in time and fourth-order accurate in space. By allowing the elastic properties and quality factors (i.e., reciprocals of attenuation) to be defined at each grid-point, realistic spatial heterogeneities may be included in the models. Note, however, that in 2-D models the guided waves and ground roll are not subject to geometrical spreading, and body (unbounded) waves spread cylindrically, whereas in reality interface waves spread cylindrically and body waves spherically.

To emulate an infinite finite-difference grid, absorbing boundaries are applied along the sides and at the base of each model, and to represent accurately the influence of surface topography, an irregular free-surface viscoelastic condition is applied at the top. The novel method for modeling topography is based on an imaging technique that produces accurate and stable results (Robertsson, 1996).

SYNTHETIC DATA

The basic viscoelastic model

Fig. 3 shows a 2-D viscoelastic model based on the preliminary interpretation of a 3-D high-resolution seismic reflection data set collected in northern Switzerland, constrained by complementary borehole and surface geological information (Lanz et al., 1996). This basic viscoelastic model is distinguished by generally low but variable Q values (i.e., relatively high attenuation) and by successive layers of (i) dry gravel and sand, (ii) saturated gravel and sand, (iii) saturated silt and sand, and (iv) saturated and compressed silt and sand. The 5 m mean thickness of the uppermost layer of dry gravel and sand is defined by the depth to the ground-water table in the survey region. This uppermost layer thus represents a waveguide with similar properties to those discussed above.

Undulating subsurface boundaries, several irregularly shaped bodies, and gentle topographic relief provide a significant measure of heterogeneity to the basic viscoelastic model (Fig. 3). According to Lanz et al. (1996), the irregular bodies (upper and lower lenses) represent either large erratic blocks, zones of anomalous compaction, or gravel channels and lenses. Interval P-velocities of the model are consistent with 3-D migration velocities from the 3-D seismic reflection data, and other material properties were estimated from appropriate Poisson's ratios and the Nafe-Drake curve (e.g. Sheriff and Geldart, 1995; Hübner et al., 1985; Bourbié et al., 1987).

The upper part of the basic viscoelastic model is shown enlarged in Fig. 4. Since the actual topography has not been surveyed with sufficient accuracy, the surface relief was chosen to be represented by a smooth fractal function with a fractal dimension of 1.1, a standard deviation from the mean elevation of 1 m, and a characteristic scale of 50 m. An inner scale was introduced by fitting a staircase-shaped function with a horizontal step size of 80 cm to the fractal function, whereas the vertical step size was limited by the finite-difference grid size. This was done for numerical reasons (Robertsson, 1996) and to quantify the potential influence of numerical scattering in convergence tests.

A source pulse with an approximate frequency content of 40 to 200 Hz (i.e., a Ricker wavelet with a 100 Hz centre frequency) was adopted for the simulations. This frequency range is similar to that of the source signal employed in collecting the experimental data presented below. In order to distinguish between the various types of source-generated noise, several properties of the basic viscoelastic model of Fig. 3 (e.g., depth to the ground-water table, degree of topographic relief, attenuation properties of the waveguide) are varied in the following simulations.

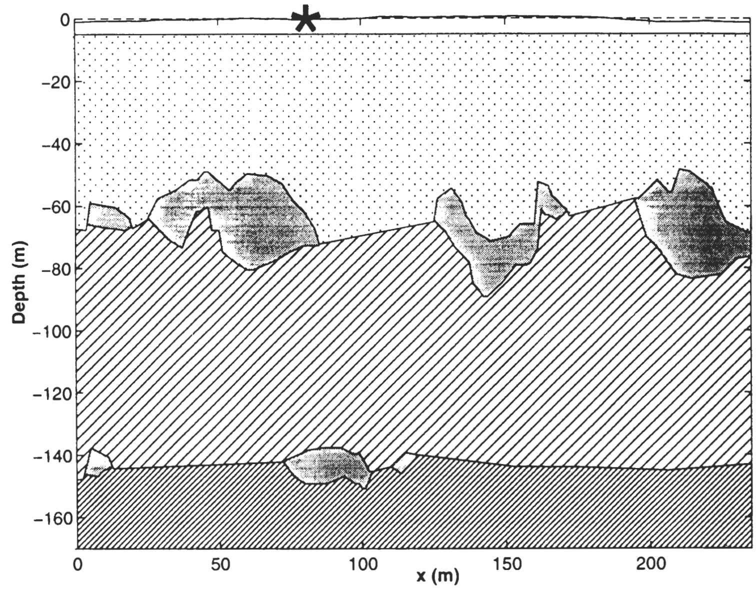

	v_p (m/s)	v_s (m/s)	ρ (kg/m³)	Q_p	Q_s
Dry gravel/sand	1100	300	1600	25/50	15/30
Wet gravel/sand	1800	400	2000	100	60
Upper lenses	2100	600	2300	250	150
Silt/sand	2000	500	2200	150	100
Lower lenses	2400	700	2500	250	150
Silt/sand	2300	600	2300	200	120

Fig. 3. 2-D velocity model for a region of northern Switzerland, based on an interpretation of a 3-D high-resolution seismic reflection data set (Lanz et al., 1996). Source location is shown by star. Material properties are listed in the legend: v_p is P-velocity, v_s S-velocity, ρ density, Q_p quality factor for P-waves, and Q_s is quality factor for S-waves. Material properties in uppermost layer of dry gravel and sand were varied in the simulations. An enlargement of near-surface region is shown in Fig. 4.

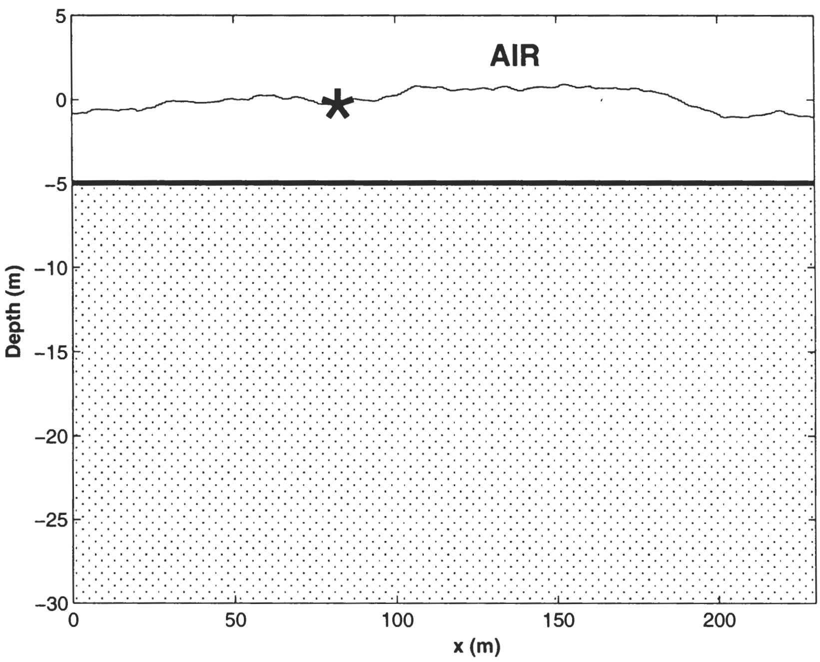

Fig. 4. Enlargement of upper part of 2-D velocity model shown in Fig. 3 showing irregular topography modeled as a smooth fractal function. Ground-water table is shown by heavy dark line. Star denotes source location. Vertical:Horizontal scale is approximately 5.

Scattering from gentle surface relief (no waveguide)

To highlight the possible influences of relatively gentle surface topography on high-resolution seismic sections, wave propagation is first simulated for a modified version of the basic viscoelastic model in which the ground-water table has been extended to the surface (i.e., there is no layer of dry gravel and sand and therefore no waveguide). Fig. 5 depicts a synthetic shot gather recorded with a 1.25 m trace interval along the top of the model. Although much weaker than the ground roll itself, events generated by scattering of the ground roll at minor surface features (Fig. 3) are clearly visible as an asymmetric criss-cross pattern in the centre of the section. Because there is no pronounced waveguide and no positive velocity gradient in the uppermost layer, the direct wave appears weak on this image. Seismic reflections cannot easily be identified at this level of scaling.

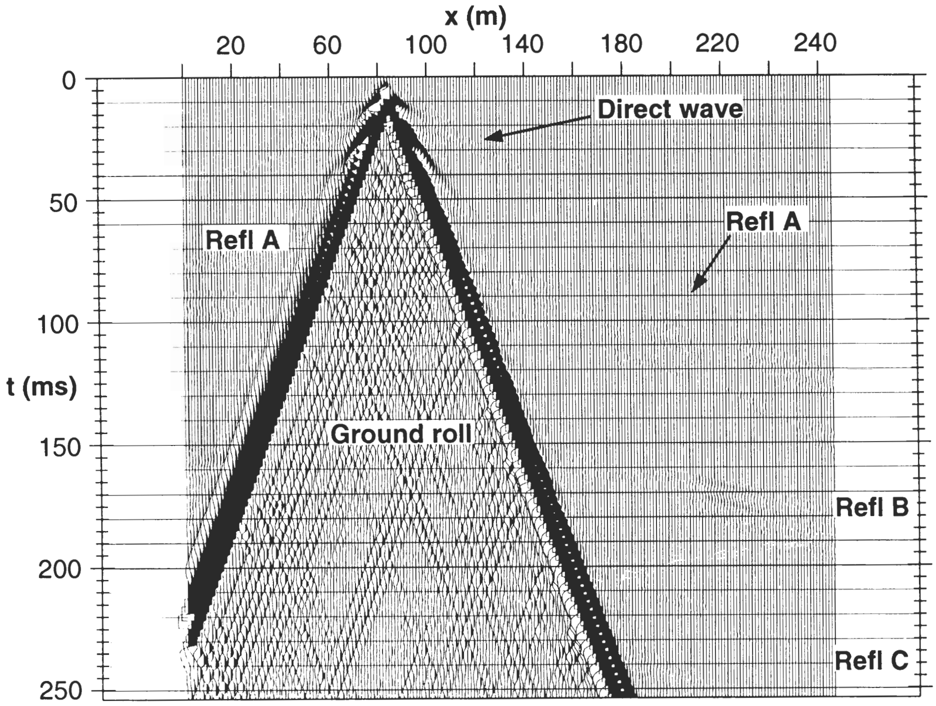

Fig. 5. Finite-difference simulation using model of Fig. 3 modified such that ground-water table extends to surface. Simulation includes effects of gentle surface relief, but since there is no layer of dry gravel and sand there is no shallow waveguide. An explosive source (100 Hz Ricker wavelet) at surface is recorded by vertical surface sensors. No distance scaling has been applied. Labels denote locations of events that cannot clearly be distinguished at this scaling. Uniform amplitude scaling factor (compare to Figs. 6, 7, 9 and 10): 8. Trace-spacing: 1.25 m.

Waveguide effects - flat free surface

By omitting the influence of topographic relief (i.e., the surface of the following model is flat), the second simulation emphasizes the effects of the near-surface waveguide (Fig. 6; Robertsson et al., 1996). Several characteristics of this synthetic shot record are observed in many high-resolution seismic sections (see Fig. 1). For example, notice the shingled and dispersed nature of the guided waves that result in a broad 'first-break' region. Shingling effects are also well known in hydrocarbon exploration and crustal-scale seismic data (Mereu et al., 1977; Sheriff and Geldart, 1995; Hurich, 1991).

Following the guided waves in Fig. 6 is a relatively quiet zone that precedes the ground roll. It is in this time range, referred to here as the 'optimum reflection window', that the clearest observations of shallow reflections are often made (see also Fig. 1). The optimum reflection window is related to the 'optimum offset' concept introduced by Hunter et al. (1984) and described in more detail by Pullan and Hunter (1990). The arrival time of the guided wavetrain is strongly dependent on the P-velocity in the waveguide. An increase in this velocity leads to earlier arrival times and an effective widening of the optimum reflection window, whereas a decrease results in later arriving guided waves and an associated narrowing of the optimum reflection window.

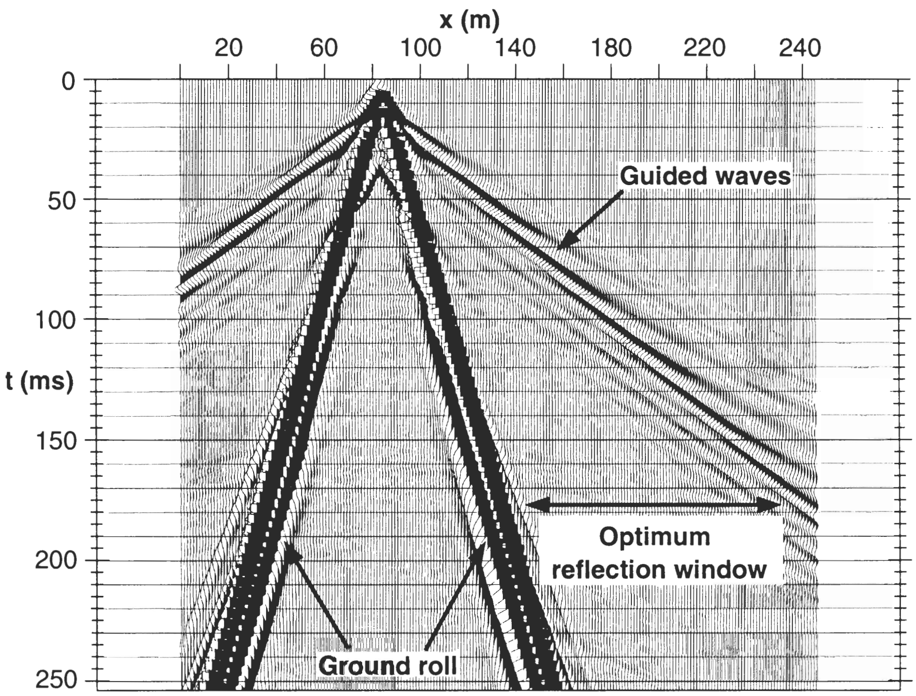

Fig. 6. Finite-difference simulation using model of Fig. 3 modified to have a flat free-surface (reproduced from Robertsson et al. (1996)); includes effects of waveguide, but not those of surface relief. An explosive source (100 Hz Ricker wavelet) at surface is recorded by vertical surface sensors. No distance scaling has been applied. Uniform amplitude scaling factor (compare to Figs. 5, 6, 9 and 10): 8. Trace-spacing: 1.25 m.

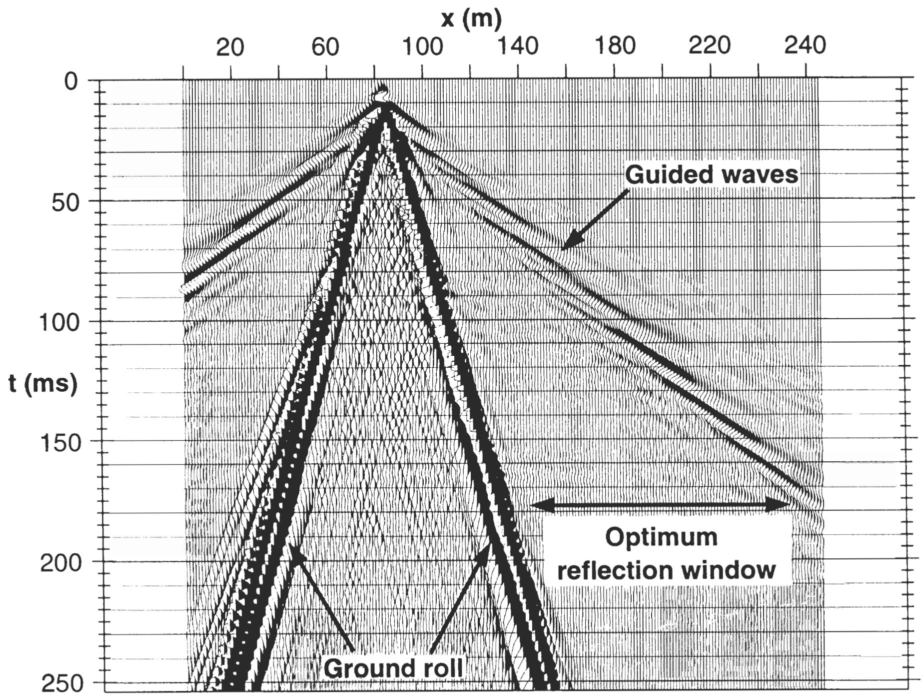

Fig. 7. Finite-difference simulation using basic viscoelastic model of Fig. 3; includes effects of waveguide and of gentle surface relief. Compare to characteristic structure of high-resolution seismic sections illustrated in Fig. 1. A surface explosive source (100 Hz Ricker wavelet) is recorded by vertical surface sensors. No distance scaling has been applied. Uniform amplitude scaling factor (compare to Figs. 5, 6, 9 and 10): 8. Trace-spacing: 1.25 m.

Waveguide effects - irregular free surface

Fig. 7 displays a shot record generated from the basic viscoelastic model of Fig. 3. By combining the effects due to the near-surface waveguide with those due to scattering at minor topographic features, this shot record reproduces well the principal features and complexity of many observed high-resolution seismic sections (Fig. 1).

Since the employed algorithm for modelling surface topography is less accurate than the finite-difference method itself (Robertsson, 1996), it is important to examine the numerical accuracy of the simulations. To test the reliability of the results presented in Fig. 7, convergence tests were performed down to a grid-spacing of 5 cm, using a grid refinement technique. A grid-spacing of 12.5 cm was found to be sufficient for the simulations presented here. Simulations based on numerous random realizations of the surface relief have been computed. An important conclusion of these tests and simulations is that the strength and shingled nature of the guided waves are not discernibly altered by the presence of gentle topographic relief. Nevertheless, scattering of the guided waves and ground roll at minor topographic features significantly increases the level of source-generated noise throughout the seismic section. Even relatively trivial topographic variations may explain both the extended coda that invariably follows the ground roll and the omni-present incoherent energy that interferes with reflections and diffractions in the optimum reflection window. Similar effects may also be generated by scattering at lateral heterogeneities within the near-surface waveguide (e.g., at large boulders, lenses of sand and gravel, faults, etc.).

Since the energy of the guided waves travels with the group velocity, near-surface velocities may be under-estimated from refraction analyses of shot records. This problem would be particularly acute if the spatial wavefield were to be inadequately sampled (i.e., aliased). Fig. 8 shows traces from the shot record of Fig. 7 plotted at 10 m intervals instead of 1.25 m.

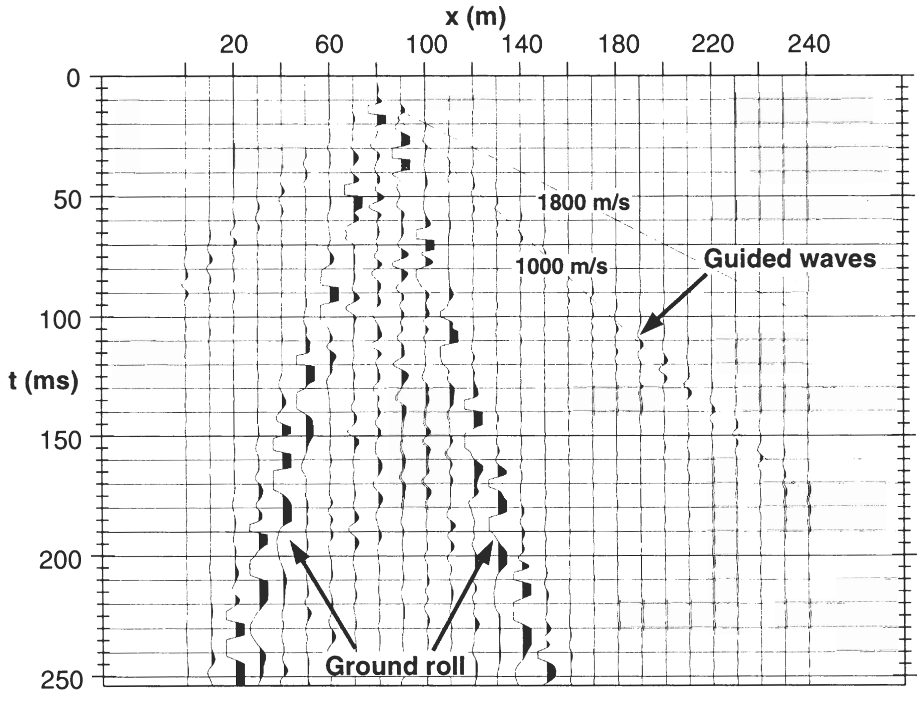

Fig. 8. Same synthetic shot record section as in Fig. 7, but with 10 m trace spacing; plotted with the same gain as Fig. 7. Solid lines show linear distance-time relationships for velocities of 1800 and 1000 m/s.

In a moderate signal-to-noise environment, a refraction analysis based on this sparsely sampled shot gather would yield an average velocity of approximately 1000 m/s for the second layer of saturated gravels and sands, which is anomalously low compared to the input velocity of 1800 m/s.

Waveguide effects - varying Q_p and Q_s within the waveguide

To display better the scattered, diffracted and reflected parts of the wavefield, traces from a portion of Fig. 7 are shown amplified in Fig. 9. The highly dispersed guided waves in these figures have a duration of about 70 ms at a distance of 200 m. There is strong interference between the incoherent scattered energy, created by the interaction of the guided waves and ground roll with the topography, and the reflections/diffractions from deeper structures; in the figure, three reflections/diffractions A, B and C have been tentatively identified as present in the observed data (see below).

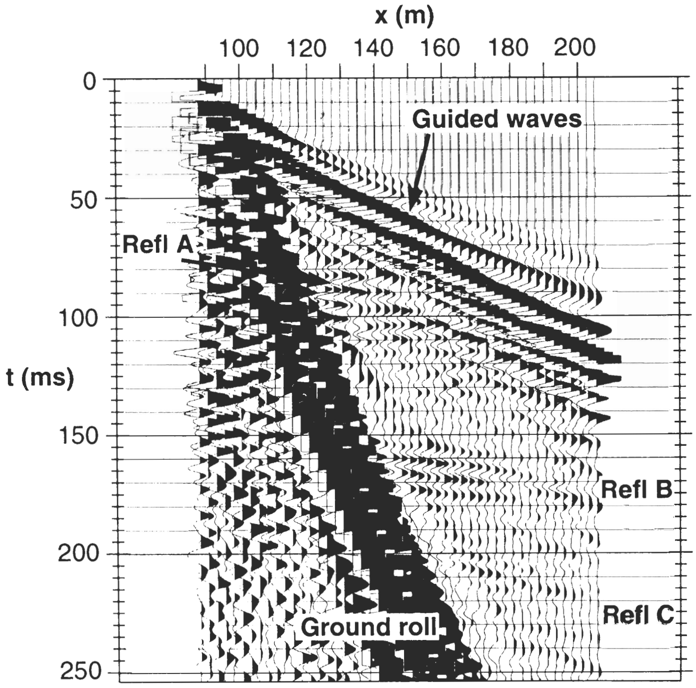

Fig. 9. Amplitude enhancement of an expanded portion of synthetic shot record shown in Fig. 7. Receiving array consists of 48 geophones equally spaced at 2.5 m intervals to right of source. No distance scaling has been applied. Uniform amplitude scaling factor (compare to Fig. 7): 90. Reflections and diffractions A, B and C mark synthetic events originating from deep interfaces and lenses.

In Fig. 10 the synthetic section obtained after halving Q_p and Q_s within the waveguide is shown; all other features of this simulation are identical to that of Fig. 9. On this shot record the guided waves and ground roll are more strongly attenuated, leading to a marked reduction in the level of scattered energy and an associated improvement in the apparent coherency of events A, B, and C. Comparison of Figs. 9 and 10 leads to a somewhat surprising conclusion: whereas high attenuation (i.e., low Q) in the shallow subsurface is undesirable from the point of view of energy penetration, it may result in a higher ratio of reflected signal to source-generated noise. There is, of course, a limit to the beneficial effects of high attenuation within the waveguide; excessive damping will eventually cause the amplitudes of desired signals (e.g., reflected phases) to fall below the ambient noise levels. On the other hand, such problems may to some extent be overcome by employing stronger sources or by averaging of multiple shot records.

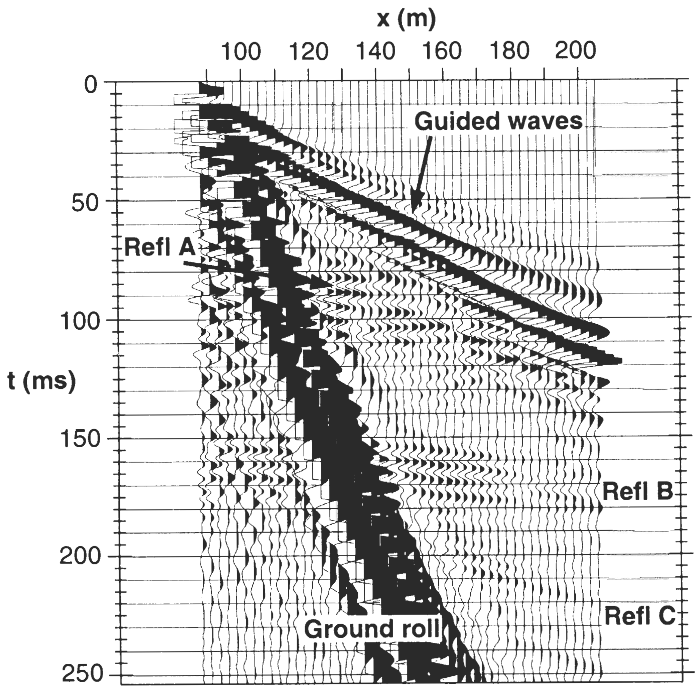

Fig. 10. As for Fig. 9, except Q values in the waveguide have been reduced to $Q_p = 25$ and $Q_s = 15$.

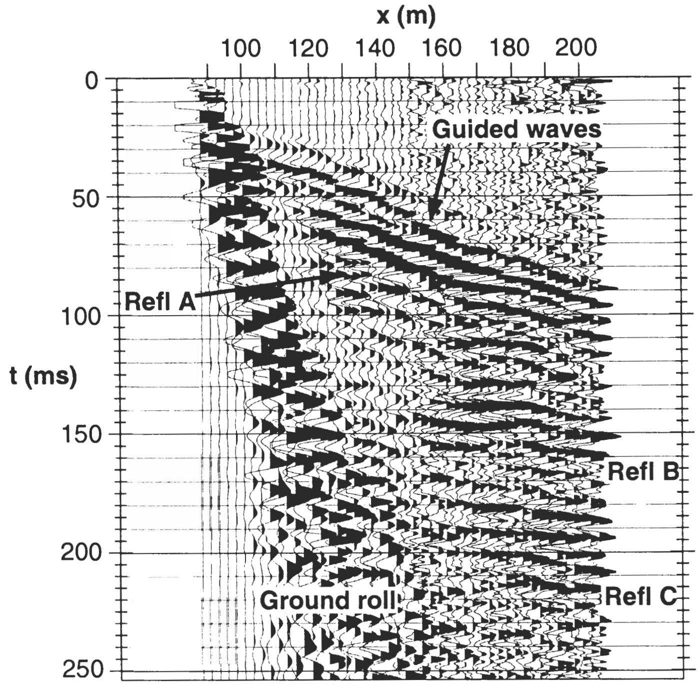

Fig. 11. Shot record from data collected in an area of northern Switzerland (reproduced from Robertsson et al., 1996; provisional model shown in Fig. 3). Complete 3-D image is shown in Lanz et al. (1996). Labelled events are approximately equivalent to those in Figs. 9 and 10. Each trace has been normalised with respect to its total energy.

COMPARISON OF SYNTHETIC AND OBSERVED SHOT RECORDS

A sample shot record from the seismic data set that led to the basic model of Fig. 3 (Lanz et al., 1996; Robertsson et al., 1996) is displayed in Fig. 11. Since the effects of guided waves and topography are the foci of this study, the basic viscoelastic model has not been tuned to match the data exactly. Regardless of this, there is a strong resemblance between the observed shot record and the synthetic one of Fig. 9. Of particular note are the similarities in the arrival times and dispersed character of the ground roll, the coda following the ground roll, and the dispersed and shingled nature of the guided waves. Both in the observed and synthetic data the genuine reflections and diffractions A, B, and C are partly obscured by the guided waves and ground roll. Although some of the earliest arrivals in the observed data could be interpreted as shallow reflections, the synthetic computations indicate that these are, instead, caused by guided waves. Problems will arise if guided waves with relatively low group velocities arrive in the same general time range as expected reflections whose stacking velocities are close to the phase velocities of the guided waves; waveguide arrivals may be mistakenly interpreted as parts of reflection-hyperbolae.

DISCUSSION AND CONCLUSIONS

Synthetic seismic sections have been generated for a variety of realistic models using a new viscoelastic finite-difference code that allows for lateral variations of velocity and attenuation and accounts for relief at the earth's free-surface. Several important conclusions can be drawn from these simulations and associated comparisons of observed and synthetic shot records:

(i) high-amplitude shingled arrivals that are common features of high-resolution seismic refraction and reflection data are probably generated by near-surface waveguides - the upper boundary of the waveguide is usually the earth's surface and its lower boundary either the ground-water table or a prominent lithological discontinuity (e.g., the unconsolidated sediment - bedrock contact);

(ii) the high-amplitudes and shingled nature of guided waves are not altered significantly by the presence of lateral heterogeneities and gentle topographic relief;

(iii) due to their dispersive nature, some guided wave phases may be mis-interpreted as shallow reflections from finely layered structures;

(iv) when guided waves arrive simultaneously with true reflections and the phase velocity in the waveguide matches the stacking velocity of the reflections, the risk for inappropriate processing and mis-interpretation is high;

(v) excitation of guided waves results in the selective frequency filtering of energy that penetrates the waveguide (equation (1); see also Robertsson et al., 1996) - using a mini-vibroseis (Matsubara et al., 1995) and similar sources it may be possible to design a source signal that either minimises the excitation of the guided waves or compensates for the selective filtering effect.

(vi) guided waves and ground roll limit the length of the optimum reflection window;

(vii) scattering of guided waves by shallow heterogeneities and minor topographic features may be important contributors to the ubiquitous source-generated noise that interferes with reflections and diffractions within the optimum reflection window and forms the long coda following the ground roll;

(viii) scattering due to shallow heterogeneities and minor topographic features are most pronounced when the near-surface waveguides are relatively low-attenuating media (i.e. $Q_p >$ approximately 50 and $Q_s >$ approximately 25); a corollary of this observation is that source-generated noise may be lower when the waveguides are relatively high-attenuating media (i.e. $Q_p <$ approximately 25 and $Q_s <$ approximately 15) so that reflections within the optimum reflection window may be easier to identify and process.

ACKNOWLEDGEMENTS

The authors thank André Pugin, Remo De Iaco, Heinrich Horstmeyer and Eva Lanz for discussions and helpful suggestions and Anne L. Blume-Robertsson for reading and helping to edit the manuscript. The authors also wish to thank Editor-in-Chief Angela Davis and two anonymous reviewers for helpful comments. The simulations were partly performed on the Cray YMP at ETH. This is ETH-Geophysics Contr. No. 885.

REFERENCES

Bourbié, T., Coussy, O. and Zinzner, B., 1987. Acoustics of Porous Media. Editions Technip, Paris, 334 pp.

Brekhovskikh, L.M., 1980. Waves in Layered Media. Academic Press, New York, 503 pp.

Hunter, J.A., Pullan, S.E., Burns, R.A., Gagné, R.M. and Good, R.L., 1984. Shallow seismic reflection mapping of the overburden-bedrock interface with the engineering seismograph - some simple techniques. Geophysics, 49: 1381-1385.

Hübner, S., Meissner, R. and Stümpel, H., 1985. Einflüsse lithologischer Parameter oberflächennaher Sedimente auf Kompressions- und Scherwellengeschwindigkeiten. In: Heitfeld, K.H. (Ed.), Ingenieurgeologische Probleme im Grenzbereich zwischen Locker- und Festgesteinen, Springer-Verlag, Berlin: 583-596.

Hurich, C.A., 1991. Source-generated noise in marine seismic profiles: The limits of reflection detectability in the upper crust. In: Meissner, R., Brown, L., Dürbaum, H., Franke, W., Fuchs, K. and Seifert, F. (Eds.), Continental lithosphere: Deep seismic reflections, Geodynamics, Vol. 22, AGU, Washington, D.C.: 443-450.

Lanz, E., Pugin, A., Green, A.G. and Horstmeyer, H., 1996. Results of 2-D and 3-D high-resolution seismic reflection surveying of surficial sediments, Geophys. Res. Let., 23: 491-494.

Matsubara, Y., Takahashi, T., Ghose, R. and Kaida, Y., 1995. Very shallow subsurface imaging using a portable vibrator. Expanded Abstr., 65th Ann. Internat. SEG Mtg., Houston, TX: 415-418.

Mereu, R.F., Epili, D. and Green, A.G., 1989. Preliminary results from the onshore GLIMPCE refraction experiment. Tectonophysics, 173: 617-626.

Mereu, R.F., Majumdar, S.C. and White, R., 1977. The structure of the crust and upper mantle under the highest ranges of the Canadian Rockies from a refraction survey. Can. J. of Earth Sciences, 14: 196-208.

Miller, R.D., Pullan, S.E., Steeples, D.W. and Hunter, J.A., 1994. Field comparison of shallow P-wave seismic sources near Houston, Texas. Geophysics, 59, 1713-1728.

Pullan, S.E. and Hunter, J.A., 1990. Delineation of buried bedrock valleys using the optimum offset shallow seismic refraction technique. In: Ward, S. (Ed.), Geotechnical and Environmental Geophysics, Vol. 3, SEG, Tulsa, OK: 75-87.

Robertsson, J.O.A., Blanch, J.O. and Symes, W.W., 1994. Viscoelastic finite-difference modeling. Geophysics, 59: 1444-1456.

Robertsson, J.O.A., 1996. A numerical free-surface condition for elastic/viscoelastic finite-difference modeling in the presence of topography. Geophysics, in press.

Robertsson, J.O.A., Holliger, K., Green, A.G., Pugin, A. and De Iaco, R., 1996. Effects of near-surface waveguides on shallow high-resolution seismic refraction and reflection data. Geophys. Res. Let., 23: 495-498.

Sheriff, R.E. and Geldart, L.P., 1995. Exploration Seismology. Cambridge University Press, Cambridge, U.K., 592 pp.

Steeples, D.W., Schmeissner, C.M. and Macy, B.K., 1995a. The evolution of shallow seismic exploration methods. J. of Environm. and Engin. Geophys., 0: 15-24.

Steeples, D.W., Macy, B.K., Schmeissner, C.M. and Miller, R.D., 1995b. Contrasting near-surface and classical seismology. The Leading Edge, 14: 271-272.

Stümpel, H., Kähler, S., Meissner, R. and Milkereit, B., 1984. The use of seismic shear waves and compressional waves for lithological problems of shallow sediments. Geophys. Prosp., 32: 662-675.

Ward, S.H., 1990. Geotechnical and Environmental Geophysics, Vol. 1-3, SEG, Tulsa, OK, 1032pp.